EPJ Web of Conferences **314**, 00023 (2024) https://doi.org/10.1051/epjconf/202431400023
QCD@Work 2024

Event shape distribution and the NLP corrections

Neelima Agarwal[1,*], *Melissa van* Beekveld[2,**], *Eric* Laenen[3,4,5,***], *Shubham* Mishra[6,7,****], *Ayan* Mukhopadhyay[6,†], and *Anurag* Tripathi[6,,‡]

[1]Department of Physics, Chaitanya Bharathi Institute of Technology, Gandipet, Hyderabad, Telangana State 500075, India
[2]Rudolf Peierls Centre for Theoretical Physics, Clarendon Laboratory, Parks Road, University of Oxford, Oxford OX1 3PU, UK
[3]Institute of Physics, University of Amsterdam, Science Park 904, 1098 XH Amsterdam, The Netherlands
[4]Nikhef, Theory Group, Science Park 105, 1098 XG, Amsterdam, The Netherlands
[5]Institute for Theoretical Physics, Utrecht University
[6]Department of Physics, Indian Institute of Technology Hyderabad, Kandi, Sangareddy, Telangana State 502285, India
[7]Department of Physics, Bharat Institute of Engineering and Technology, Mangalpally, Ibrahimpatnam, Hyderabad, Telangana State, 501510, India

Abstract. For the event shapes thrust and c-parameter at next-to-leading order, we examine the origins of next-to-leading power corrections. We track down the origin of these factors for each shape of the event and compare our findings with a recent method that makes use of the eikonal approximation and momentum changes derived from the Low-Burnett-Kroll-Del Duca theorem. We do an analytical and numerical analysis of the differences. Both precise and approximate findings are described in terms of elliptic integrals for the c-parameter; yet, it exhibits patterns that are similar to those observed in the thrust results near the elastic limit.

1 Introduction

In perturbative QCD, precise cross-section estimates must be obtained at the same rate as collider-physics observations get more precise. Two contrasting approaches are used in this endeavor. Initially, precise higher-order computations in the coupling α_s are performed, and pertinent techniques are developed. Second, under particular kinematic limits, when certain classes of logarithmic terms become strengthened, all-order results are achieved. There are numerous methods that can be used to resum these logarithmic terms to any order, and their variety keeps growing. This holds true in particular for the near-elastic zone, also known as the threshold region, where the phase space of emitted particles is bounded. In such a

*e-mail: dragarwalphysics@gmail.com
**e-mail: melissa.vanbeekveld@physics.ox.ac.uk
***e-mail: eric.laenen@nikhef.nl
****e-mail: shubhamhere82@gmail.com
†e-mail: ayanmukhopadhyay5@gmail.com
‡e-mail: tripathi@phy.iith.ac.in

situation, the cancellation of infrared singularities, guaranteed by the KLN theorem [1, 2] leaves large logarithmic remainders at any order in perturbation theory. To be more specific, if ξ is a dimensionless kinematic variable, such that $\xi \to 0$ towards the elastic region, the corresponding differential cross-section has the generic form

$$\frac{d\sigma}{d\xi} = \sum_{n=0}^{\infty} \left(\frac{\alpha_s}{\pi}\right)^n \left[\sum_{m=0}^{2n-1} c_{nm}^{\rm LP} \left(\frac{\log^m \xi}{\xi}\right)_+ + c_n^{(\delta)} \delta(\xi) + \sum_{m=0}^{2n-1} c_{nm}^{\rm NLP} \log^m \xi + \ldots\right]. \tag{1}$$

The first term on the right in the above equation is well-known to originate from soft and/or collinear radiation and, together with the second term, makes up the *leading power* (LP) terms. Much is known about LP terms to arbitrary order, and there have been numerous approaches towards their resummation and power correction studies. The last term on the right corresponds to terms that are *next-to-leading power* (NLP). These are produced via collinear gluon, soft quark/anti-quark, and soft gluon emissions (next to). Even if they are supressed by a power of ξ, the growth of these logarithmic terms towards threshold makes them numerically relevant for the precision studies. The exact arrangement of these NLP terms to all orders and arbitrary logarithmic accuracy is yet unclear, in contrast to the LP terms. In this work [3], we focus on such NLP terms for two event shapes in e^+e^- collisions: thrust [4, 5] and the C-parameter [6]. The calculation at NLO for spherocity can be found in [7]. These observables are interesting in this regard because in contrast to most of the previous studies in direct QCD, all QCD effects reside in the final state, and because their definition involves special phase space constraints that were not considered so far. For these observables, our aim is to trace the origin of the NLP terms near the elastic limit, to examine to what extent there is a common pattern of NLP terms, and assess their size. Here we examine to what extent NLP terms for two event shapes can be predicted using the kinematical shift method, as well as the soft quark emission approximation [8, 9].

The leading logarithmic terms can alternatively be computed using the approach of shifted kinematics [10], in this approach the matrix element that can capture terms up to NLP at NLO is given by the formula

$$\overline{\sum}|\mathcal{M}|^2 = g_s^2 N_c (N_c^2 - 1) \frac{2p_1 \cdot p_2}{(p_1 \cdot p_3)(p_2 \cdot p_3)} |\mathcal{M}_0(p_1 - \delta p_1, p_2 - \delta p_2)|^2 , \tag{2}$$

where $|\mathcal{M}_0(p_1, p_2)|^2$ is the matrix element squared at the leading order (LO), and $\overline{\sum}$ denotes the sum (average) over the final (initial) state spins and colours, p_3 is the momentum of the emitted radiation, and p_1, p_2 are the momenta of the particles already present at the Born level. The shifts in the momenta are given by

$$\delta p_1^\mu = -\frac{1}{2}\left(\frac{p_2 \cdot p_3}{p_1 \cdot p_2} p_1^\mu - \frac{p_1 \cdot p_3}{p_1 \cdot p_2} p_2^\mu + p_3^\mu\right), \; \delta p_2^\mu = -\frac{1}{2}\left(\frac{p_1 \cdot p_3}{p_1 \cdot p_2} p_2^\mu - \frac{p_2 \cdot p_3}{p_1 \cdot p_2} p_1^\mu + p_3^\mu\right). \tag{3}$$

Expressions (2) and (3) yield the dominant NLP contributions to the NLO matrix element.

2 Event shape distribution

In this work the process taken under consideration, and shown in figure below is

$$e^+(p_b) + e^-(p_a) \to \gamma^*(q) \to q(p_1) + \overline{q}(p_2) + g(p_3)\,. \tag{4}$$

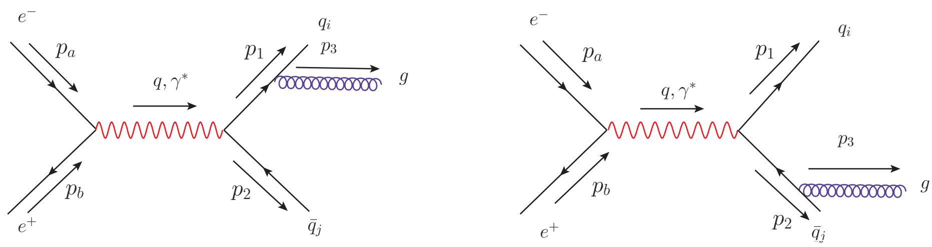

Figure 1. Feynman diagrams for the real emission of a gluon.

The event shape distribution at NLO has the form

$$\frac{d\sigma}{dX} = \frac{1}{2s}\int d\Phi_3 \overline{\sum} |\mathcal{M}(x_1, x_2)|^2 \delta(X - X(x_1, x_2, x_3))\,, \tag{5}$$

where s is the center of mass energy squared, and $d\Phi_3$ is the three-body phase space factor. The scaleless energy fraction variables x_i are defined for each parton as

$$x_i = \frac{2E_i}{Q}\,, \tag{6}$$

where E_i is the energy of i^{th} parton, and Q is the centre of mass energy. The energy fraction variables satisfy the constraint $x_1 + x_2 + x_3 = 2$. The matrix element squared for the process in eq. (4) is

$$\overline{\sum} |\mathcal{M}(x_1, x_2)|^2 = 8(e^2 e_q)^2 g_s^2 C_F N_c \frac{1}{3Q^2}\left[\frac{x_1^2 + x_2^2}{(1 - x_1)(1 - x_2)}\right], \tag{7}$$

where $\alpha = \left(e^2/4\pi\right)$, e_q is the charge of quarks in the unit of fundamental electric charge e, $\alpha_s = g_s^2/4\pi$, $C_F = (N_c^2 - 1)/2N_c$, and N_c is the number of quark colours. The two event shape variables that we are going to study in this work are thrust and C-parameter. Thrust is defined as

$$T = \max_{\hat{\mathbf{n}}} \frac{\sum_i |\mathbf{p_i} \cdot \hat{\mathbf{n}}|}{\sum_i E_i}\,. \tag{8}$$

For a final state with three massless particles, eq. (8) takes the simple form

$$T = \max\{x_1, x_2, x_3\}\,. \tag{9}$$

The C-paramter is given by

$$C = 3 - \frac{3}{2}\sum_{i,\,j} \frac{\left(p_i \cdot p_j\right)^2}{(p_i \cdot q)\left(p_j \cdot q\right)}\,. \tag{10}$$

For our process, we define a rescaled c-parameter, the expression for which is

$$c \equiv \frac{C}{6} = \frac{(1 - x_1)(1 - x_2)(1 - x_3)}{(2 - x_1 - x_2)(2 - x_2 - x_3)(2 - x_1 - x_3)}\,. \tag{11}$$

We are going to use the above expressions of thrust and c-parameter[1] (rescaled c parameter instead of C-parameter) to compute their respective event shape distribution in upcoming sections.

2.1 Thrust distribution

To obtain the thrust distribution one integrates over the x_1, x_2 variables in eq. (5) with the appropriate limits:

$$\frac{1}{\sigma_0(s)}\frac{d\sigma}{dT} = \frac{2\alpha_s}{3\pi}\int_0^1 dx_1 \int_0^{1-x_1} dx_2 \, \frac{x_1^2+x_2^2}{(1-x_1)(1-x_2)} \times \delta(T-\max(x_1,x_2,x_3)) \tag{12}$$

where $x_3 = 2 - x_1 - x_2$, and $\sigma_0(s)$ is the LO cross-section. For our purposes, we categorize the contributions from three different regions of the phase space integration in eq. (12). These regions are defined by which of x_1, x_2, or x_3 is the largest, and we refer to them as region-I, region-II, and region-III, respectively. The contribution from region I is then

$$\frac{1}{\sigma_0(s)}\frac{d\sigma}{dT}\bigg|_{\mathrm{I}} = \frac{2\alpha_s}{3\pi}\int_0^1 dx_2 \int_0^{1-x_2} dx_1 \, \frac{x_1^2+x_2^2}{(1-x_1)(1-x_2)} \, \delta(T-x_1)\,. \tag{13}$$

Instead of T, we shall mostly use the variable $\tau = 1 - T$, which vanishes in the zero-radius dijet limit. Upon integrating and expanding around $\tau = 0$

$$\frac{1}{\sigma_0(s)}\frac{d\sigma}{d\tau}\bigg|_{\mathrm{I}} = \frac{2\alpha_s}{3\pi}\Big(\frac{-3-4\log\tau}{2\tau} + 2\log\tau + \frac{3\tau}{2} - \tau\log\tau + O(\tau^2)\Big). \tag{14}$$

Region-I captures the leading log (LL) at LP and NLP both. In region II, due to the symmetry under the interchange of $x_1 \leftrightarrow x_2$, the contribution from this region is identical to eq. (14). Thus

$$\frac{1}{\sigma_0(s)}\frac{d\sigma}{d\tau}\bigg|_{\mathrm{II}} = \frac{2\alpha_s}{3\pi}\Big(\frac{-3-4\log\tau}{2\tau} + 2\log\tau + \frac{3\tau}{2} - \tau\log\tau + O(\tau^2)\Big). \tag{15}$$

In region III, the thrust axis is aligned with the momentum of the gluon. The contribution is given by

$$\frac{1}{\sigma_0(s)}\frac{d\sigma}{dT}\bigg|_{\mathrm{III}} = \frac{2\alpha_s}{3\pi}\int_0^1 dx_2 \int_0^{1-x_2} dx_1 \, \frac{x_1^2+x_2^2}{(1-x_1)(1-x_2)} \, \delta(T+x_1+x_2-2)\,. \tag{16}$$

Integrating and expanding in τ gives

$$\frac{1}{\sigma_0(s)}\frac{d\sigma}{d\tau}\bigg|_{\mathrm{III}} = \frac{2\alpha_s}{3\pi}\Big(-2-2\log\tau + (2-2\log\tau)\tau + O(\tau^2)\Big). \tag{17}$$

The region-III captures only the LL at NLP, and no contributions from LP gets captured here. Combining the contributions from these three regions we finally get

$$\frac{1}{\sigma_0(s)}\frac{d\sigma}{d\tau}\bigg|_{\mathrm{NLO}} = \frac{2\alpha_s}{3\pi}\Big(\frac{-3-4\log\tau}{\tau} - 2 + 2\log\tau + (5\tau - 4\log\tau)\tau + O(\tau^2)\Big). \tag{18}$$

[1] $c = C/6$

Note that in eq. (18) at NLP all three regions produce LL terms, but a partial cancellation takes place when combined.

The expression of matrix element squared under shifted formalism for our process derived using eq. (2) reads as

$$\overline{\sum}|\mathcal{M}_{\rm shift}(p_1, p_2)|^2 \ = \ 8(e^2 e_q)^2 N_c g_s^2 C_F \, \frac{1}{3Q^2} \left(\frac{2x_1 + 2x_2 - 2}{(1-x_1)(1-x_2)}\right) . \tag{19}$$

The result of thrust distribution in region-I using fomalism of shifts results in

$$\frac{1}{\sigma_0(s)} \frac{d\sigma}{d\tau}\bigg|_{\rm I} \ = \ \frac{2\alpha_s}{3\pi} \left(\frac{-2 - 2\log\tau}{\tau} + 2 + 2\log\tau + \mathcal{O}(\tau^2)\right) . \tag{20}$$

When we compare the above expression to eq. (14), we see that the LLs at both the LP and NLP are correctly captured, while the NLL terms at LP are only partially reproduced. Similarly the contribution from region-III for small values of τ is given as

$$\frac{1}{\sigma_0(s)} \frac{d\sigma}{d\tau}\bigg|_{\rm III} \ = \ \frac{2\alpha_s}{3\pi}\Big(- 4\tau\log\tau + \mathcal{O}(\tau^2)\Big). \tag{21}$$

This is as expected, as the hard gluon/soft quark region is not part of the shifted kinematics method. Combining contributions from all three regions the thrust distribution from shifted kinematics formalism at NLO reads or

$$\frac{1}{\sigma_0(s)} \frac{d\sigma}{d\tau}\bigg|_{\rm shift} \ = \ \frac{2\alpha_s}{3\pi}\Big[\frac{-4 - 4\log\tau}{\tau} + 4 + 4\log\tau - (4\log\tau)\tau + \mathcal{O}(\tau^2)\Big]. \tag{22}$$

The LL at LP are captured correctly, however LL at NLP are only captured partially.

In order to find the remaining LLs we use the soft quark approximation, the expression of matrix element squared in this approximation is

$$\overline{\sum}|\mathcal{M}_{\rm rem}(x_1, x_2)|^2 \ = \ 8(e^2 e_q)^2 N_c C_F g_s^2 \frac{1}{3Q^2}\Big(\frac{1-x_2}{1-x_1} + \frac{1-x_1}{1-x_2}\Big). \tag{23}$$

Thrust distribution computed from soft quark approximation results in

$$\frac{1}{\sigma_0(s)} \frac{d\sigma}{d\tau}\bigg|_{\rm rem} \ = \ \frac{2\alpha_s}{3\pi}\Big(\frac{1}{\tau} - 6 - 2\log\tau + 5\tau\Big). \tag{24}$$

Thus we notice that the soft quark approximation captures the remaining logarithmic terms at the LP and NLP for thrust distribution. The above expression when combined with shifted kinematics result in eq. (22) produces all the terms of thrust distribution given in eq. (18).

2.2 C-parameter distribution

The c-parameter distribution for the process under consideration is given by the expression

$$\frac{1}{\sigma_0(s)} \frac{d\sigma}{dc} \ = \ \frac{1}{2s} \int d\Phi_3 \, \overline{\sum}|\mathcal{M}(x_1, x_2)|^2 \, \delta(c(y,z) - c) \, . \tag{25}$$

where the expression of matrix element squared and c-parameter in terms of new set of variables y and z is given by

$$\sum |\mathcal{M}(y,z)|^2 = 8(e^2 e_q)^2 N_c C_F g_s^2 \frac{1}{3Q^2}\left(\frac{2+y(y-2yz(1-z)-2)}{y^2 z(1-z)}\right), \tag{26}$$

and

$$c(y,z) = \frac{(1-y)(1-z)yz}{(1-y(1-z))(1-yz)}\,. \tag{27}$$

The new variables are defined as

$$\begin{aligned} y &= 2 - x_1 - x_2\,, \\ z &= \frac{1-x_2}{y}\,, \end{aligned} \tag{28}$$

The expression for c-parameter distribution as given in eq. (25) upon substituting the above expressions of matrix element squared and c-parameter reads as

$$\frac{1}{\sigma_0(s)}\frac{d\sigma}{dc}\bigg|_{\text{NLO}} = \frac{2\alpha_s}{3\pi}\int_0^1 dy \int_0^1 dz \frac{2(y(z-1)+1)^2(yz-1)^2(y(2y(z-1)z+y-2)+2)}{(y-1)^2 y^2 (z-1)z(2z-1)} \times\Big(\delta(z-z_1)+\delta(z-z_2)\Big). \tag{29}$$

After the z integration the limits of y change to (y_1, y_2), see below in eq. (31). We have now

$$\frac{1}{\sigma_0(s)}\frac{\mathrm{d}\sigma}{\mathrm{dc}}\bigg|_{\text{NLO}} = \frac{2\alpha_s}{3\pi}\int_{y_1}^{y_2} dy \frac{2(1-y)(y\left(c(y-2)^2+(y-3)y+4\right)-2)}{c(cy+y-1)\sqrt{y(cy+y-1)\left(c(y-2)^2+(y-1)y\right)}}\,. \tag{30}$$

$$y_1 = \frac{1+4c-\sqrt{1-8c}}{2(1+c)}\,, \qquad y_2 = \frac{1+4c+\sqrt{1-8c}}{2(1+c)}\,. \tag{31}$$

The integration over y in eq. (30) produces incomplete elliptic integrals of three types, each with somewhat involved arguments and coefficients. After conversion to their so-called complete counterparts and carefully collecting their coefficients, the final expression can be organized in a compact form as follows

$$\frac{1}{\sigma_0(s)}\frac{d\sigma}{dc}\bigg|_{\text{NLO}} = \frac{2\alpha_s}{3\pi}\Big(e(c)\,\mathrm{E}[m_1(c)] + p(c)\,\Pi[n_1(c), m_1(c)] + k(c)\,\mathrm{K}[m_1(c)]\Big), \tag{32}$$

where E, Π, and K are the standard complete elliptic integrals of the first, second, and third kind. The arguments of these elliptic integrals in eq. (32) have the following form

$$n_1(c) = \frac{2\sqrt{1-8c}}{1+\sqrt{1-8c}-4c}\,, m_1(c) = \frac{2\sqrt{1-8c}}{1+\sqrt{1-8c}-4c-8c^2}\,. \tag{33}$$

The arguments have monotonic behavior. The elliptic integrals in eq. (32) have the following asymptotic behavior as $c \to 0$

$$\begin{aligned} \mathrm{E}[m_1(c)] &= 1 + \mathcal{O}(c^3 \log c)\,, \\ \Pi[n_1(c), m_1(c)] &= -\frac{\log c}{8c^2} + \frac{6\log c - 3}{8c} + \frac{15 - 8\log c}{16} + \frac{9\log c + 10}{3}c + \mathcal{O}(c^2)\,, \\ \mathrm{K}[m_1(c)] &= -\frac{3\log c}{2} + \mathcal{O}(c^3 \log c)\,. \end{aligned} \tag{34}$$

The expression for the coefficients appearing in eq. (32) around $c = 0$ are

$$\begin{aligned} e(c) &= -\frac{3}{c} + 9 + 12c + 36c^2 + O(c^3)\,, \\ p(c) &= 32c + 112c^2 + O(c^3)\,, \\ k(c) &= 4 - 20c + 48c^2 + O(c^3)\,. \end{aligned} \tag{35}$$

From eqs. (33), (34) and (35) the c-parameter distribution at NLO for small-c reads,

$$\frac{1}{\sigma_0(s)}\frac{d\sigma}{dc}\bigg|_{\rm NLO} = \frac{2\alpha_s}{3\pi}\bigg(\frac{-3-4\log c}{c} - 3 + 4\log c + O(c)\bigg). \tag{36}$$

We next compute the c-parameter distribution using the shifted kinematics method, and again assess to what extent LP and NLP terms in the exact NLO calculation are reproduced. The approximation is The shifted matrix element in eq. (19), when written in terms of the transformed variables (y, z), takes the form

$$\overline{\sum}|\mathcal{M}_{\rm shift}(y,z)|^2 = 8(e^2 e_q)^2 N_c C_F g_s^2 \frac{1}{3Q^2}\left(\frac{2(y-1)}{y^2(z-1)z}\right). \tag{37}$$

After the z integration we have

$$\frac{1}{\sigma_0(s)}\frac{d\sigma}{dc}\bigg|_{\rm shift} = \frac{2\alpha_s}{3\pi}\int_{y_1}^{y_2} dy \frac{4(y-1)^2}{c\sqrt{y\,(y+cy-1)\,(c(y-2)^2+(y-1)y)}}\,. \tag{38}$$

The above integral again results in to elliptic integrals as given in eq. (32). The small-c behavior of coefficients of elliptic integrals obtained in this case are

$$\begin{aligned} e_{\rm s}(c) &= -\frac{4}{c} + 16 - 4c + 72c^2 + O(c^3)\,, \\ p_{\rm s}(c) &= 32c + 128c^2 + O(c^3)\,, \\ k_{\rm s}(c) &= -8c + O(c^3)\,. \end{aligned} \tag{39}$$

Using these results, the expression of c-paramter distribution at NLO up to NLP is given by

$$\frac{1}{\sigma_0(s)}\frac{d\sigma}{dc}\bigg|_{\rm shift} = \frac{2\alpha_s}{3\pi}\bigg(\frac{-4-4\log c}{c} + 4 + 8\log c + O(c)\bigg). \tag{40}$$

On the other hand the expression obtained from soft quark approximation reads as

$$\frac{1}{\sigma_0(s)}\frac{d\sigma}{dc}\bigg|_{\rm rem} = \frac{2\alpha_s}{3\pi}\left(\frac{1}{c} - 7 - 4\log c + O(c)\right). \tag{41}$$

Thus we notice from the two expressions above that the shifted approach along with the soft quark approximation reproduces the LL up to NLP at NLO accurately.

3 Conclusions

Fixed-order studies in perturbative QCD face challenges from IR singularities, which persist even after cancellation, leaving logarithmic corrections behind. These logarithms, categorized as LL and NLL at different powers, including LP and NLP, must be resummed to derive meaningful results from these studies. We calculated these logarithms with the primary aim of determining the LL at NLP for the event shape distributions of thrust and c-parameter. We found that combining the shifted approach with the soft quark approximation effectively captured the LL up to NLP. This method can be applied to other event shape variables and processes to evaluate the accuracy of the shifted approach and to identify the significant LL at NLP for resummation purposes.

References

[1] T. Kinoshita, A. Ukawa, Mass Singularities of Feynman Amplitudes, Lect. Notes Phys. **39**, 55 (1975). 10.1007/BFb0013300

[2] T.D. Lee, M. Nauenberg, Degenerate Systems and Mass Singularities, Phys. Rev. **133**, B1549 (1964). 10.1103/PhysRev.133.B1549

[3] N. Agarwal, M. van Beekveld, E. Laenen, S. Mishra, A. Mukhopadhyay, A. Tripathi, Next-to-leading power corrections to event-shape variables, Pramana **98**, 60 (2024), 2306.17601. 10.1007/s12043-024-02743-0

[4] E. Farhi, A QCD Test for Jets, Phys. Rev. Lett. **39**, 1587 (1977). 10.1103/PhysRevLett.39.1587

[5] S. Catani, G. Turnock, B.R. Webber, L. Trentadue, Thrust distribution in e+ e- annihilation, Phys. Lett. B **263**, 491 (1991). 10.1016/0370-2693(91)90494-B

[6] J.F. Donoghue, F.E. Low, S.Y. Pi, Tensor Analysis of Hadronic Jets in Quantum Chromodynamics, Phys. Rev. D **20**, 2759 (1979). 10.1103/PhysRevD.20.2759

[7] S. Mishra, Next-to-leading power corrections to spherocity distribution at NLO in QCD (2024), 2403.16449

[8] M. van Beekveld, W. Beenakker, E. Laenen, C.D. White, Next-to-leading power threshold effects for inclusive and exclusive processes with final state jets, JHEP **03**, 106 (2020), 1905.08741. 10.1007/JHEP03(2020)106

[9] M. van Beekveld, W. Beenakker, E. Laenen, A. Misra, C.D. White, The role of soft quarks in next-to-leading power threshold effects, PoS **RADCOR2019**, 053 (2019). 10.22323/1.375.0053

[10] V. Del Duca, E. Laenen, L. Magnea, L. Vernazza, C.D. White, Universality of next-to-leading power threshold effects for colourless final states in hadronic collisions, JHEP **11**, 057 (2017), 1706.04018. 10.1007/JHEP11(2017)057